

# Thin films of aluminum nitride and aluminum gallium nitride for cold cathode applications

Cite as: Appl. Phys. Lett. **71**, 2289 (1997); <https://doi.org/10.1063/1.120052>

Submitted: 23 April 1997 • Accepted: 15 August 1997 • Published Online: 05 August 1998

A. T. Sowers, J. A. Christman, M. D. Bremser, et al.



View Online



Export Citation

## ARTICLES YOU MAY BE INTERESTED IN

[Properties of aluminum nitride thin films for piezoelectric transducers and microwave filter applications](#)

Applied Physics Letters **74**, 3032 (1999); <https://doi.org/10.1063/1.124055>

[Electrical properties of atomic layer deposited aluminum oxide on gallium nitride](#)

Applied Physics Letters **99**, 133503 (2011); <https://doi.org/10.1063/1.3645616>

[GaN, AlN, and InN: A review](#)

Journal of Vacuum Science & Technology B: Microelectronics and Nanometer Structures Processing, Measurement, and Phenomena **10**, 1237 (1992); <https://doi.org/10.1116/1.585897>

QBLOX



1 qubit

Shorten Setup Time  
**Auto-Calibration**  
**More Qubits**

Fully-integrated  
**Quantum Control Stacks**  
**Ultrastable DC to 18.5 GHz**  
Synchronized <<1 ns  
Ultralow noise



100s qubits

[visit our website >](#)

# Thin films of aluminum nitride and aluminum gallium nitride for cold cathode applications

A. T. Sowers, J. A. Christman, M. D. Bremser, B. L. Ward, R. F. Davis,  
and R. J. Nemanich

*Department of Physics and Department of Materials Science and Engineering, North Carolina State University, Raleigh, North Carolina 27695-8202*

(Received 23 April 1997; accepted for publication 15 August 1997)

Cold cathode structures have been fabricated using AlN and graded AlGa<sub>x</sub>N structures (deposited on *n*-type 6H-SiC) as the thin film emitting layer. The cathodes consist of an aluminum grid layer separated from the nitride layer by a SiO<sub>2</sub> layer and etched to form arrays of either 1, 3, or 5  $\mu\text{m}$  holes through which the emitting nitride surface is exposed. After fabrication, a hydrogen plasma exposure was employed to activate the cathodes. Cathode devices with 5  $\mu\text{m}$  holes displayed emission for up to 30 min before failing. Maximum emission currents ranged from 10–100 nA and required grid voltages ranging from 20–110 V. The grid currents were typically 1 to 10<sup>4</sup> times the collector currents. © 1997 American Institute of Physics. [S0003-6951(97)01242-4]

The electrical properties of wide bandgap semiconductors in combination with the high temperature chemical stability make these materials candidates for use in high power and high frequency devices. Moreover, wide bandgap semiconductors such as diamond AlN,<sup>1,2</sup> and Al<sub>x</sub>Ga<sub>1-x</sub>N for  $x \geq 0.75$ <sup>3</sup> show promise for use as cold cathode materials since these materials have been observed to exhibit a negative electron affinity (NEA).

The presence of a negative electron affinity for wide bandgap semiconductors means that electrons excited into the conduction band can be freely emitted into the vacuum. Prior studies that detected the presence of a NEA for these materials employed ultraviolet (UV) photoexcitation. Thus, carriers excited into the conduction band near the surface could escape and be detected. In contrast, for field emission from a NEA material, if electrons can be supplied to the conduction band then they would be freely emitted into the vacuum. An ideal wide bandgap semiconductor would then exhibit a NEA and also sufficient *n*-type doping to supply electrons into the conduction band and to form low resistance contacts. To date, it has proved difficult to produce an *n*-type wide bandgap NEA semiconductor. While *n*-type GaN is routinely obtained by Si doping, *n*-type characteristics of AlN have not been confirmed.

Much wide bandgap field emission research has been dedicated to depositing diamond on various field emitting tips<sup>4,5</sup> or depositing selectively grown GaN pyramids on *n*-type 6H-SiC.<sup>6,7</sup> Indeed, some research has been dedicated to using diamond films for field emission device applications.<sup>8,9</sup> Previous experiments from our laboratories show that field emission from nitride materials exhibits Fowler–Nordheim behavior similar to that from diamond.<sup>10</sup> Our approach then is to use a planar nitride surface as the emitter rather than a structure that deliberately exploits field enhancement at a sharp projection. The advantage of this approach is that sputtering and other tip degradation processes are avoided. This approach is similar to recently fabricated diamond cathodes.<sup>11</sup>

The basic approach employed in this study is presented in the nitride cold cathode design shown in Fig. 1. An aluminum grid is separated from the nitride emitting layer by a

SiO<sub>2</sub> layer. An array of square emission holes is etched through the aluminum and SiO<sub>2</sub> to the nitride layer. At the bottom of the emission hole, the electron emission occurs at the vacuum–nitride interface induced by the grid voltage ( $V_g$ ) between the aluminum pad and the backside contact.

Two different nitride emitting layer structures are employed. In one structure a thin AlN layer is deposited on an *n*-type 6H-SiC substrate. In this case, electrons from the SiC would be extracted through the AlN layer. AlN has a direct bandgap of 6.2 eV while 6H-SiC has an indirect bandgap of 3.0 eV. The heterojunction conduction band offset between

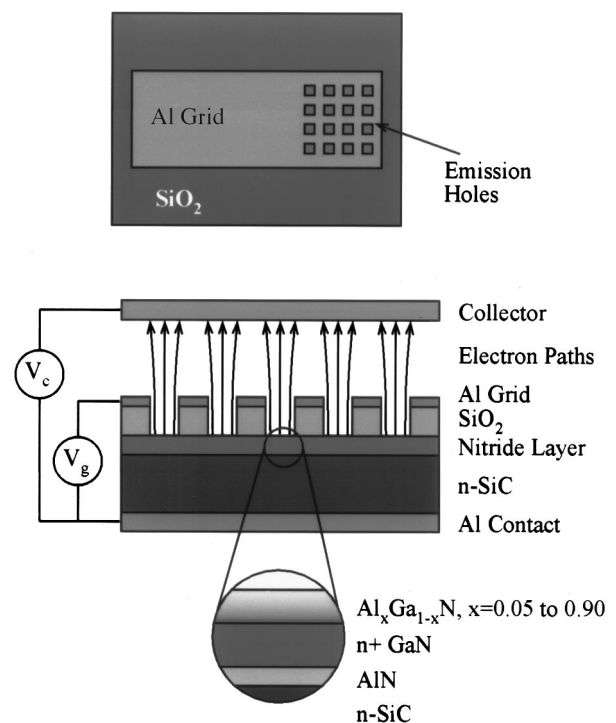


FIG. 1. Schematic of the cold cathode structures. The top view shows a 5  $\times$  5 array of emission holes. The Al grid is 1  $\times$  2 mm, the emission holes are either 1, 3, or 5  $\mu\text{m}$ , and the hole spacing varies from 5 to 75  $\mu\text{m}$ . The nitride layer is exposed through the holes. The schematic cross section (bottom) is across the emission holes. The inset shows the nitride layers used in the graded AlGa<sub>x</sub>N devices.

the AlN and SiC is expected to be between 1.8 to 2.4 eV with the conduction band of the AlN above that of the SiC.<sup>2</sup> The second approach involves an *n*-type GaN base layer with an Al<sub>x</sub>Ga<sub>1-x</sub>N graded layer. This graded layer varies in composition from  $x=0.05$  at the interface with the GaN base layer to  $x=0.90$  at the emitting surface. Electrons are supplied to the *n*-type GaN and then emitted through the NEA Al rich AlGa<sub>x</sub>N layer. If the grading is completely smooth then there would be no sharp barriers for the conduction electrons.

Prior to patterning, the nitride emitting layer is deposited on a 6H-SiC substrate using the metalorganic chemical vapor deposition system described elsewhere.<sup>12,13</sup> The first structure employed a 1000 Å AlN layer deposited directly on the SiC substrate. The second structure uses a 1000 Å AlN buffer layer deposited on the SiC substrate. The *n*+GaN base layer is grown on this buffer layer and is 1 μm thick doped to  $n=1\times10^{19}\text{ cm}^{-3}$  with silicon. The graded Al<sub>x</sub>Ga<sub>1-x</sub>N layer is 0.5 μm thick and is graded from  $x=0.05$  to  $x=0.90$ . The surfaces of both nitride emitting layers are expected to exhibit a NEA.<sup>2</sup> As shown by atomic force microscopy, the nitride films are smooth with root mean square roughness of ~20 Å on a 1×1 μm scan. However, cracking of the top surface was observed by scanning electron microscopy (SEM) for the graded AlGa<sub>x</sub>N emitting layer. The cracks were ~0.1 μm wide with an average domain size of 5 μm<sup>2</sup> between cracks.

Fabrication of the cold cathodes is accomplished with a two mask process. A SiO<sub>2</sub> layer (~1 μm thick) is deposited on the nitride layer at 400 °C by low pressure chemical vapor deposition using diethylsilane and oxygen precursors. The grid layer is formed with 200–300 nm of thermally evaporated aluminum. The first mask step creates the emission holes which are either 1, 3, or 5 μm squares. Square holes were used for convenience of the lithography system. The aluminum is patterned with a standard aluminum etch. Reactive ion etching (RIE) (with SF<sub>6</sub> and O<sub>2</sub>) is used to etch the oxide in order to obtain high aspect ratio features. Since the RIE environment may damage the emitting surface, a wet oxide etch is used to etch the last ~0.1 μm of oxide to expose the nitride layer. The second mask step defines the 1×2 mm metal pads that form the grids. The last processing step is thermal evaporation of 200–300 nm of aluminum onto the backside of the SiC to form an electrical contact.

The electrical testing system has two electrical probes. One probe is used to make contact to the grid and the other probe is used to collect the emission current ~1 mm above the holes. In this configuration only the total emission current for a single device is obtained. The grid voltage can be varied from 0–110 V and the collector voltage from 0–1100 V using two Keithley source measure units (SMUs). The SMU can simultaneously source a voltage and measure the current through the circuit. The maximum current is limited by the compliance value which was 1 μA for the collector probe and 10 or 100 mA for the grid probe. The pumping system is oil free and testing is performed at pressures <5 × 10<sup>-7</sup> Torr.

The nitride cathodes were electrically tested directly after processing and no collector or grid currents above the noise level were measured for the several devices tested. It

was determined that a post processing clean was necessary to activate emission from the nitride cathodes. Since the aluminum grids are exposed, we are limited to cleans which will not etch away the grids or damage the nitride layer. The samples were cleaned ultrasonically in methanol for 10 min and then subjected to a remote hydrogen plasma clean at 25 mTorr and 450 °C for 10 min. A hydrogen plasma exposure with these parameters has been shown to remove hydrocarbons from AlN and GaN surfaces.<sup>14</sup> Also, a hydrogen plasma will remove residual photoresist. After plasma exposure, the sample is immediately transported in air to the electrical testing system.

Both AlN and AlGa<sub>x</sub>N cathode structures exhibited collector currents well above the current background level. Only cathodes with 5 μm emission holes displayed emission, and the cathode lifetimes varied from several up to 30 min. For all measurements shown in this article, the grid and collector currents were measured at a constant grid voltage while the collector voltage was varied. These measurements were repeated at different grid voltages for each device. This procedure was employed to verify that it was indeed the grid voltage that induced the emission. No significant direct dependence on collector voltage was observed, but the emission signal varied significantly at different times. At a constant grid voltage, the varying collector current is attributed to cathode instability rather than to the changing collector voltage.

Identical structures but without emission holes were also fabricated to test the SiO<sub>2</sub> properties. These test structures are on the same wafer as the cathodes, and therefore undergo the exact same processing and plasma treatments. The oxide breakdown voltage for these structures was found to be >800 V which is much higher than the grid voltages of 0–110 V used during normal cathode testing. No collector currents above the noise level have been measured for the structures without emission holes.

Figure 2(a) shows the average current–voltage data for four cathodes that operated for ~30 min. As expected, the collector current ( $I_c$ ) increases with increasing grid voltage. The collector current and grid current ( $I_g$ ) were essentially independent of the collector voltage and depended mainly upon the grid voltage as shown in Fig. 2(b). This AlGa<sub>x</sub>N cathode had the largest collector current of the graded film devices measured ( $I_c \cong 10$  nA). Grid currents for the AlGa<sub>x</sub>N devices were 10<sup>3</sup> to 10<sup>4</sup> times the collector current. The electrical measurement was improved and the noise base line was reduced for the AlN devices. Similar data was obtained from the AlN cathodes with the ratio of the grid current to the collector current ranging from 1–100.

The cathodes that functioned followed similar patterns during testing. Initially, the grid current would be high, either 10 or 100 mA, depending on the SMU compliance value, and no emission was detected at the collector. Then the grid current would drop and a collector current could be measured. SEM of the cathodes after testing revealed evidence of melting of the aluminum grid layer around the emitting holes and at the point of contact between the aluminum pad and the grid probe. The emission holes would be enlarged and rounded, and sometimes more severely damaged. This effect is attributed to either current flowing along the

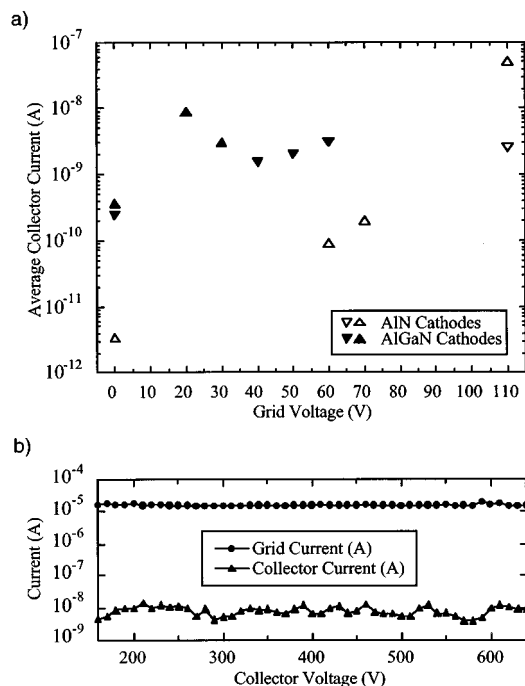


FIG. 2. (a) Current–voltage characteristics for four cathode devices. The open and closed triangular markers represent data obtained from devices with the thin AlN emitting layer and the graded AlGaIn emitting layer, respectively. The up and down triangles are associated with different devices. The electrical measurements were improved for the AlN devices which lowered the noise base line. (b) Grid and collector currents obtained from an AlGaIn cathode with  $V_g = 20$  V.

sidewalls of the emission holes or electrons emitted from the nitride surface and then collected on the aluminum grid. We suspect that after the H-plasma clean, a conducting residue coats the sides of the emission holes. This creates a short between the grid and the nitride layer. During initial device testing, a high current flows through the residue which eventually decomposes the residue, and the current may also melt areas of the grid around the holes. After this decomposition occurs, an electric field can build up at the nitride surface and electron emission is detected. We also suspect that the devices with 1 and 3  $\mu\text{m}$  holes do not function because of residue that remains after processing.

It is difficult to make a quantitative comparison between the two nitride emitting layers. This is primarily due to the limited lifetime of the devices. As a result, data was not obtained from all devices under identical voltage conditions. In general, the AlGaIn devices required lower grid voltages than the AlN devices to begin operating. However, once emission was achieved, similar collector currents were obtained for both emitting layers. In addition, the high grid currents obtained preclude a Fowler–Nordheim analysis of the collected current.

We suggest several changes for improved operation of the nitride cathode devices. The AlN buffer layer required for high quality growth may be a significant barrier for the emission particularly from the graded films. A top contact type structure in which the electron supply contact is made to the  $n$ -type GaN layer would circumvent this problem. It is also apparent that improved fabrication processes are necessary. In addition further studies are required on the effect of various surface treatments on the electron emission from AlN or AlGaIn layers.

The authors express their appreciation to the NCSU Microelectronic Fabrication Laboratory staff for help with the lithography and processing necessary to fabricate the cathodes. We acknowledge Bill Partlow of Northrup-Grumman for additional field emission measurements and for helpful discussions. We also thank Chris Hatfield and Griff Bilbro for helpful discussions and device simulations. This research is supported by the Office of Naval Research and the Northrup-Grumman Science and Technology Center.

- <sup>1</sup>J. van der Weide and R. J. Nemanich, Phys. Rev. B **49**, 13629 (1994).
- <sup>2</sup>M. C. Benjamin, C. Wang, R. F. Davis, and R. J. Nemanich, Appl. Phys. Lett. **64**, 3288 (1994).
- <sup>3</sup>M. C. Benjamin, M. D. Bremser, J. T. W. Weeks, S. W. King, R. F. Davis, and R. J. Nemanich, Appl. Surf. Sci. **104/105**, 455 (1996).
- <sup>4</sup>E. I. Givargizov, J. Vac. Sci. Technol. B **13**, 414 (1995).
- <sup>5</sup>J. Liu, V. V. Zhirnov, G. J. Wojak, A. F. Myers, W. B. Choi, J. J. Hren, S. D. Wolter, M. T. McClure, B. R. Stoner, and J. T. Glass, Appl. Phys. Lett. **65**, 2842 (1994).
- <sup>6</sup>O. H. Nam, M. D. Bremser, B. L. Ward, R. J. Nemanich, and R. F. Davis, *III–V Nitrides*, edited by F. A. Ponce, T. D. Moustakas, I. Akasaki, and B. A. Monemar, Mater. Res. Soc. Proc. 449 (Materials Research Society, Pittsburgh, PA, 1997), pp. 107–112.
- <sup>7</sup>R. D. Underwood, D. Kapolnek, B. P. Keller, S. Keller, S. P. DenBaar, and U. K. Mishra, Topical Workshop on Nitrides, Nagoya, Japan, September (1995).
- <sup>8</sup>N. S. Xu, Y. Tzeng, and R. V. Latham, J. Phys. D **27**, 1988 (1994).
- <sup>9</sup>M. W. Geis and J. C. Twichell, Appl. Phys. Lett. **67**, 1–4 (1995).
- <sup>10</sup>R. J. Nemanich, M. C. Benjamin, S. W. King, M. D. Bremser, R. F. Davis, B. Chen, Z. Zhang, and J. Bernholc, *GaN and Related Materials*, edited by F. A. Ponce, R. D. Dupuis, S. Nakamura, and J. A. Edmond, Mater. Res. Soc. Proc. 395 (Materials Research Society, Pittsburgh, PA, 1996) pp. 375–380.
- <sup>11</sup>M. W. Geis, J. C. Twichell, N. N. Efremow, K. E. Krohn, C. Marchi, and T. M. Lyszczarz, *Proceedings of the 8th International Vacuum Microelectronics Conference* (unpublished, 1995), p. 277.
- <sup>12</sup>M. D. Bremser, W. G. Perry, N. V. Edwards, T. Zheleva, N. Parikh, D. E. Aspnes, and R. F. Davis, Mater. Res. Soc. Symp. Proc. **395**, 195 (1996).
- <sup>13</sup>M. D. Bremser, W. G. Perry, T. Zheleva, N. V. Edwards, O. H. Nam, N. Parikh, D. E. Aspnes, and R. F. Davis, MRS Internet J. Nitride Semicond. Res. **1**, 8(1996).
- <sup>14</sup>S. W. King, L. L. Smith, J. P. Barnak, J. Ku, J. A. Christman, M. C. Benjamin, M. D. Bremser, R. J. Nemanich, and R. F. Davis, in *GaN and Related Materials*, edited by F. A. Ponce, R. D. Dupuis, S. Nakamura, and J. A. Edmond, Mater. Res. Soc. Proc. 395 (Materials Research Society, Pittsburgh, PA, 1996), pp. 739–744.